Supplemental Information for J. Aoto et al., "**Presynaptic Neurexin-3 Alternative Splicing Trans-Synaptically Controls Postsynaptic AMPA-Receptor Trafficking**"

SUPPLEMENTARY FIGURE LEGENDS

Supplementary Figure S1

Quantitative rt-PCR standard curves for Nrx1, Nrx2, and Nrx3 SS4 variants (A), intrinsic electrical membrane properties of WT and of constitutive Nrx3-SS4+ and Nrx3-SS4- neurons (B), mEPSC and mIPSC parameters (C-F), and paired-pulse ratio measurements (G) as a function of defined Nrx3 SS4 variants (related to Fig. 1)

(A) Quantitative validation of rt-PCR assays for measuring Nrxn1, Nrxn2, and Nrxn3 mRNAs containing (top) or lacking (bottom) an insert in SS#4. Standard qRT-PCR curves with probes that detect the insert at SS4 of neurexin-1 (left), neurexin-2 (middle), and neurexin-3 (right). All standard curves have R^2 values of 0.999 (n=4 independent runs).
(B) Intrinsic electrical properties (membrane resistance, top, and membrane capacitance, bottom) of hippocampal neurons that were cultured from wildtype or conditional $Nrx3^{SS4+}$ mice and infected with lentivirus expressing inactive ($Nrx3^{SS4+}$) or active cre-recombinase ($Nrx3^{SS4-}$).
(C) Cumulative distributions of the frequency (left) and amplitude (right) of mEPSCs monitored in hippocampal neurons that were cultured from wild-type or conditional $Nrx3^{SS4+}$ mice, infected with lentivirus expressing inactive ($Nrx3^{SS4+}$) or active ($Nrx3^{SS4-}$) cre-recombinase.
(D) Analysis of the mEPSC kinetics. Absolute and scaled traces (left) and average mEPSC rise and decay times (right) are shown.
(E) and (F) Same as C and D, but for mIPSCs. In F, only absolute representative mIPSC traces are shown since the mIPSC amplitudes of WT and Nrx3-SS4+ and Nrx3-SS4- neurons are undistinguishable.
(G) Test for changes in presynaptic release probability in hippocampal neurons that were cultured from WT mice or from conditional $Nrx3^{SS4+}$ mice, and infected with lentivirus expressing inactive ($Nrx3^{SS4+}$) or active cre-recombinase ($Nrx3^{SS4-}$). NMDA-receptor mediated EPSCs were measured to avoid network activity. Representative traces are shown on the left, the paired-pulse ratio observed with 200 ms interstiumulus interval in the middle, and a plot of the paired-pulse ratio as a function of increasing (40 ms to 2 s) inter-stimulus intervals on the right.

Data in B, D, F, and G are means ± SEM (numbers in bars indicate number of cells/cultures analyzed). Data in C and E show cumulative distribution of all data pointes obtained in three independent cultures from the number of cells indicated in D and F, respectively. Statistical significance was evaluated by the K-S test (C and E) or single-factor ANOVA (D, F, and G), with *, $p<0.05$; **, $p<0.01$; ***, $p<0.001$. Non-significant comparisons are not identified

Supplementary Figure S2

Protocol used for analysis of surface AMPA-type GluA1 and GluA2 receptors (A), normalized and absolute values for the quantifications of surface GluA1 and GluA2 and of intracellular excitatory synapse markers (PSD-95 and vGluT1) in WT, $Nrx3^{SS4+}$ and $Nrx3^{SS4-}$ neurons (B & C), and protocol used for measuring GluA1 endocytosis (D) (related to Fig. 3)

(A) Schematic flow diagram of GluA1 surface and intracellular labeling methodology.

(B) Normalized values for synapse quantification parameters shown in Fig. 3 in neurons cultured from wildtype mice or from conditional $Nrx3^{SS4+}$ mice, infected with active ($Nrx3^{SS4-}$) or inactive ($Nrx3^{SS4+}$) cre recombinase. The top bar graphs show the normalized density (left) and size (right) of PSD95 and vGluT1 immunoreactive puncta. The lower bar diagram represents the normalized intensity of GluA1, GluA2, PSD95, or vGluT1 puncta.
(C) Absolute values for synapse quantification parameters shown in Fig. 3. The left bar diagram shows the absolute quantification of surface GluA1, GluA2, PSD-95 and vGluT1 immunoreactive puncta density (per 10μm of dendrite), the middle bar diagram represents the absolute intensity (arbitrary units) and the right bar diagram shows the absolute puncta sizes (μm^2) for the same markers measured in hippocampal neurons that were cultured from WT or conditional $Nrx3^{SS4+}$ mice and infected with lentivirus expressing inactive (retains the splice-site insert = $Nrx3^{SS4+}$) or active cre-recombinase (removes the splice site insert = $Nrx3^{SS4-}$). Numbers in bars = number of independent experiments.
(D) Schematic flow diagram detailing the GluA1 internalization assay.

Data shown in B and C are means ± SEM; statistical analysis was performed by single-factor ANOVA (number in graphs = number of independent cultures analyzed; *, $p<0.05$; **, $p<0.01$; non-significant comparisons are not identified).

Supplementary Figure S3

Characterization of regular- and burst-firing pyramidal neurons of the subiculum in acute hippocampal slices (A), and analysis of paired-pulse ratios in regular and burst-firing subicular neurons 2-3 weeks after stereotactic injection of AAVs into the CA1 region of the hippocampus *in vivo* (B and C)(related to Fig. 5)

AAVs were injected at P21 into the CA1 region of the dorsal hippocampus. WT mice were injected with AAVs encoding GFP, whereas $Nrx3^{SS4+}$ mutant mice were injected with AAVs encoding inactive ($Nrx3^{SS4+}$-$CA1^{Ctrl}$) or active cre-recombinase ($Nrx3^{SS4+}$-$CA1^{Cre}$). The AAVs only infect the CA1 region and not the subiculum (see Fig. 5A), and this procedure thus specifically manipulates presynaptic inputs at the CA1-subiculum synapse. Acute hippocampal slices were cut from injected mice 2-3 weeks later at P35-42 mice, and depolarizing steps in current-clamp configuration identified burst- and regular-firing subicular neurons (see panel A). Paired-pulse ratios (B and C) were acquired in voltage-clamp mode.
(A) Representative traces identifying postsynaptic regular- (top) or burst-firing (bottom) neurons in the subiculum following increasing depolarization. Inset shows burst firing in response increasing depolarization.
(B) Comparison of EPSC paired-pulse ratios of regular (left) or burst firing subicular neuons (right) following alveus stimulation (CA1) at given inter-stimulus intervals ranging from 20 ms to 2 s.
(C) Same data as B, but plotted as a comparison of regular firing with burst-firing neurons.

Data shown in B and C are means ± SEM; n = number of cells recorded; statistical significance was determined by single-factor ANOVA; *, $p<0.05$.

Supplementary Figure S4

LTP control experiments (A), representative raw data for LTP measurements (B), and LTP-dependent changes in presynaptic release probability (C) (related to Fig. 6)

(A) Summary graphs of whole-cell recordings of LTP control experiments in regular and burst firing cells in the subiculum of acute hippocampal slices cut from WT P35-42 mice as described in Fig. S3. As in Fig. 6, LTP was induced by 4 x 100 Hz tetani applied by stimulation of CA1 axons in the alveus while in current-clamp mode at resting membrane potential. EPSCs were sampled at 0.1 Hz while in voltage-clamp configuration. Recordings were performed after application of 100 μm D-APV to ensure that the LTP observed is NMDAR-dependent.
(B) Representative LTP experiments monitored in burst (top) and regular firing subicular neurons (bottom) in acute slices obtained from WT mice 2-3 weeks after in vivo introduction of GFP-expressing AAVs, and from $Nrx3^{SS4+}$ mice 2-3 weeks after in vivo introduction of control AAVs (*$Nrx3^{SS4+}$-$CA1^{Ctrl}$*) or cre-recombinase expressing AAVs (*$Nrx3^{SS4+}$-$CA1^{Cre}$*). LTP was induced and monitored as described for A.
(C) Summary graph of paired-pulse ratios (PPRs) measured in burst (top) and regular firing subicular pyramidal neurons (bottom). PPRs were monitored 10 min before (Pre-LTP) and 60 min after LTP induction (Post-LTP). Postsynaptic EPSCs were evoked by extracellular stimulation of the alvear pathway at given inter-stimulus intervals. Slices were obtained as described for B.

Data shown in A and C are means ± SEM; n = number of cells recorded; statistical significance was determined by single-factor ANOVA; **, $p<0.01$; *, $p<0.05$.

Supplementary Figure S5

Measurements of the surface levels of LRRTM2 and neuroligin-1 (NL1) in cultured WT, $Nrx3^{SS4+}$, or $Nrx3^{SS4-}$ hippocampal neurons (related to Fig. 7)

(A) Normalized values for the intensity of LRRTM2 and NL1 immunoreactive puncta in Fig. 7 in neurons cultured from wildtype or conditional $Nrx3^{SS4+}$ mice, infected with active ($Nrx3^{SS4-}$) or inactive ($Nrx3^{SS4+}$) cre recombinase.
(B) Cumulative probability plot representing NL1 puncta size for WT, $Nrx3^{SS4+}$ and $Nrx3^{SS4-}$ cultured hippocampal neurons.
(C) Summary graphs representing the absolute quantification values of LRRTM2 and NL1 immunoreactive puncta in neurons cultured from wildtype mice or from conditional $Nrx3^{SS4+}$ mice, infected with active ($Nrx3^{SS4-}$) or inactive ($Nrx3^{SS4+}$) cre recombinase. The left graph shows the average puncta density (per 10μm of dendrite), the middle graph shows the average puncta intensity (arbitrary units) and the right graph shows the average puncta size (μm^2). Number in bars = number of independent experiments.

Data in A and C are means ± SEM; statistical significance was determined by single-factor ANOVA; *, $p<0.05$.

DETAILED METHODS

Generation of mutant mice. *Nrx3*$^{SS4+}$ mutant mice were generated by homologous recombination in R1 embryonic stem cells (Tabuchi et al., 2007) using the strategy outlined in Fig. 1B that targets the alternatively spliced SS4-exon 20 of *Nrxn3* (Tabuchi and Südhof, 2002). Following homologous recombination, positive clones were validated by Southern blotting and PCR genotyped and were injected into C57BL/6 blastocysts. The *Nrx3*$^{SS4+}$ mouse line was obtained after flp-recombinase mediated deletion of the neo cassette in the germ line, while the *Nrx3*$^{SS4-}$ mouse line was produced by cre-recombinase mediated deletion of exon 20 in the germ line of *Nrx3*$^{SS4+}$ mutant mice as described (Kaeser et al., 2011). Genotyping was performed using the following primers: for Nrx3^{SS4+}: CTCCAACCTGTCATTCAAGGG and CTACGGGCCGGTTATATTTG (300 bp product) and for Nrx3^{SS4-}: CTCCAACCTGTCATTCAAGGG and CTGAATGCACCAGGGTATCAC (425 bp product). All mouse work was performed as prescribed by approved protocols at Stanford, and the original mouse line was submitted to Jackson Labs for distribution.

Measurements of neurexin SS4+ and SS4- mRNA levels in mouse brain. RT-PCR on brain tissues was performed on RNA isolated from P21 mice and from DIV14-16 hippocampal cultures using the RNAqueous-Micro RNA isolation kit (Invitrogen). 80 ng of total RNA was added to each reaction using the LightCycler 480 reagent kit (Roche). Reactions were run and analyzed using a 7900HT Fast RT-PCR instrument (Applied Biosystems) with β-actin as the endogenous internal control. All real time PCR PrimeTime assays were custom designed through Integrated DNA Technologies. Custom gene expression assays (Nrx1^{SS4+}: primers ACAGCTGGCCAGTTATCGAACGCT/AGCT GACGCCCTTTGTCGAGTAGCCATT and probe AATGATAACGAGCGCCTGGCGATTGCTA; Nrx1^{SS4-}: primers TACCCTGCAGGGCGTCA/GCCATATTCAGAACTTTCAAGCC and probe CACA ATCTTCAATAGCCAAGCAACCATAA; Nrx2^{SS4+}: primers TGAGCGACGGCAAATATCAC/ACTA CTCGACCAAGCCGGTA and probe ACCACTTCGAGTAAAGCGCACCA; Nrx2^{SS4-}: primers GACG GCAAATATCACGTGGTGCGCT/TCAGCTGGCGTCCTGCCGG and probe AATGCCACCTTG CAAGTGGACAGCT; Nrx3^{SS4+}: primers TACGGGCCGGTTATATTTG/TGGCCAGTGAATGAGC AC and probe CAGGCAACACTGATAATGAACGCCTCCAAAT; Nrx3^{SS4-}: primers AGAGAACTC CTGTCAATGATG/TTAGCTGCCGGCCTGTA and probe CAAATACCACGTTGTGCGCTTCACCA GGAATG) were used.

Cloning of rescue constructs. Mouse Nrx3α cDNAs containing inserts at SS1 and SS3, which correspond to the inclusion of the alternative exons 2 and 3 (SS1) and exon 11 (SS3), and lacking inserts in SS2 and SS5, were isolated from a mouse brain cDNA library using the following primers: F: 5'-ATATAGATCTGCCACCATGAGCTTTACCCTCCACTCA-3'; R: 5'-ATATCAATTGT TACACATAATACTCCTTGTC-3'. The Nrx3α cDNAs in- or excluded SS4. Mouse Nrx1β, Nrx2β, and Nrx3β cDNAs containing or lacking an insert in SS4 but lacking an insert in SS5 were isolated from a mouse brain cDNA library using the following primers: For Nrx1β: F: 5'-ATATGGATCCG CCACCATGTACCAGAGGATGCTTCGGT-3'; R: 5'-ATATCAATTGTCAGACGTAATACTCCTTA TC-3'. For Nrx2β: F: 5'-ATATGGATCCGCCACCATGCCCTTCCTCACCCGCAG-3'; R: 5'-ATATGA ATTCTCAGACGTAATACTCTTTGTC-3'. For Nrx3β: F: 5'-ATATGCTAGCAAAAAAGCCACCATG AGCTTTACCCTCCACTCA-3'; R: 5'-ATATCAATTGTTACACATAATACTCCTTGTC-3'. All cDNAs were cloned into the lentiviral vector FSW and used for rescue experiments as described in Fig. 2.

Antibodies. The following primary antibodies were used in this study: PSD95 (ICC: 1:200; mouse monoclonal; Affinity Bioreagents, Golden, CO), GluA1 (ICC: 1:4; rabbit polyclonal; Calbiochem,

San Diego, CA); GluA2 (ICC 1:30: mouse monoclonal; Milipore); LRRTM2 (ICC: 1:30; rabbit polyclonal; Santa Cruz Biotechnology, Inc.); NL1 (ICC: 1:75; rabbit polyclonal; Santa Cruz Biotechnology, Inc.); vGluT1 (ICC: 1:500; guinea pig polyclonal; Millipore, Temecula, CA). The following secondary polyclonal antibodies were used: anti-rabbit AlexaFluor488 (1:500), anti-rabbit AlexaFluor546, anti-mouse AlexaFluor546 (1:500), and anti-guinea pig AlexaFluor633 (1:500) (all from Invitrogen, San Diego, CA).

AMPAR imaging experiments. **GluA1 and GluA2 surface labeling** was performed as described (Aoto et al., 2008; Carroll et al., 1999; Lin et al., 2000). Briefly, culture neurons were washed with PBS containing 0.5 mM $CaCl_2$ and 1 mM $MgCl_2$ (PBS^{MC}) with 4% sucrose. Neurons were preincubated at 37° C for 5 min with primary antibodies against GluA1 to allow labeling of surface AMPA receptors, washed with ice-cold PBS^{MC}, fixed with 4% PFA + 4% sucrose for 15 minutes, then blocked in a detergent-free blocking solution (PBS with 2% normal goat serum (Sigma, St. Louis, MO), and 0.02% sodium azide) for 1 hr, followed by secondary antibody incubation at room temp for 1 hour. To immunolabel for excitatory synaptic markers, cultures were then postfixed with -20°C methanol for 1 min to permeabilize the neurons. Cells were blocked in blocking solution for 1 hr, followed by incubation with primary antibodies for PSD95 and vGluT1. Neurons were washed and incubated with a secondary antibody at room temp for 1 hr, mounted, and imaged. **LRRTM2 and NL1 surface labeling** was performed on neurons fixed with 4% PFA + 4% sucrose for 15 minutes, then blocked in detergent-free blocking solution for 1 hr. Fixed neurons were immunostained under non-permeablized conditions for 1 hr at room temperature before application of secondary antibody. **AMPAR GluA1 internalization assays** were essentially performed as described (Lin et al., 2000). Live hippocampal neurons at 14-16 days in vitro were labeled at 37°C for 5 min with a primary antibody against an extracellular epitope of GluA1 to allow labeling of surface AMPA receptors. Cells were washed in PBS^{MC} then incubated at 37°C with neuron growth media for 15-20 minutes to allow for basal internalization. Cells were then washed and fixed with 4% PFA/4% sucrose, blocked in a detergent-free blocking solution for 1 hr, followed by an AlexaFluor488 secondary antibody incubation at room temp for 1hr to label the surface population. Neurons were then postfixed with 100% methanol at -20°C and stained with an AlexaFluor546 secondary antibody to immunolabel the pre-labeled internalized fraction. To calculate the percent internalization, the integrated red fluorescence intensity, identifying internalized GluA1, was divided by the total (red + green) intensity. **Image acquisition and quantification** were performed as described (Aoto et al., 2007; Aoto et al., 2008). Cells were chosen at random from three or more independent cultures. Images were taken from at least three coverslips per experiment. Fluorescent images were acquired at room temperature with an Olympus (Tokyo, Japan) FV1000 BX61WI laser-scanning confocal microscope using an Olympus Plan Apochromat 60x oil objective (NA: 1.42; WD: 0.15) set to 3x zoom with sequential acquisition, averaging of 3 frames, and set to 1024x1024 pixel resolution. Laser power and photomutiplier settings were set so bleedthrough was negligible between channels. Within the same experiment, the same settings for laser power, PMT gain, and offset were used. These settings provided images where the brightest pixels were just under saturation. Digital images were taken using the Olympus Fluoview Imaging software (Olympus). 7-12 0.5 μm optical sections were used and maximum pixel intensity projections were created. For quantifications, images were thresholded by intensity to exclude background signals and puncta were quantified by counting the number of puncta whose areas ranged from 0.1-4.0 μm^2. For each experiment, at least 15 cells per condition were analyzed and the mean and SEM

were calculated. Data shown represent the average of the mean values from at least 3 independent experiments.

Viral constructs and preparation of viruses. All lentiviruses used in the present study employ previously described vectors (Kaeser et al., 2011) in which we exchanged the ubiquitin-C promoter with a human synapsin promoter (Südhof, 1990). All analyses in cultured neurons employed matched sets of lentiviruses expressing either mutant cre-recombinase (control) or active cre-recombinase (to convert *Nrx3*$^{SS4+}$ neurons into *Nrx3*$^{SS4-}$ neurons); both the mutant control and the active cre-recombinase included enhanced For cre-recombinase localization signals to render them indistinguishable and completely nuclear (Kaeser et al., 2011). All rescue constructs were mouse cDNAs expressed from separate lentiviruses. Lentiviruses were produced by co-transfection of HEK293T cells with third generation helper plasmids (VSVG, pRSV-REV, and pMDLg/pRE) using the calcium phosphate method (Kaeser et al., 2011; Pang et al., 2011; Xu et al., 2012). Lentiviral particles were harvested 48 h after transfection, spun at 500 x g for 5 min to pellet cellular debris, and added to cultured neurons.

For in vivo infections, we employed the AAV-DJ strain that is highly efficient in vivo (Xu et al., 2012). AAV vectors were constructed from an empty cloning vector where the expression cassette is as follows: left-ITR of AAV2, CMV promoter and beta-globin intron, multiple cloning site (MCS), hGH poly A sequence and right ITR. eGFP, inactive (GFP-ΔCre) and active (GFP-Cre) cre-recombinase were inserted into the multiple cloning sites. AAV plasmids were co-transfected with pHelper and pRC-DJ into HEK293T cells. 72 h post transfection, cells were harvested, lysed and run on an iodixanol gradient by ultracentrifugation at 400,000g for 2 h. The 40% iodixanol fraction containing AAV was collected, concentrated and washed in a 100K MWCO ultracon filter. Purified AAVs were titered by infecting HEK-293T cells with serial dilutions, and used for stereotaxic infections at 1 x 10^7 infectious units/μl.

Analysis of cultured hippocampal neurons. Hippocampal neurons were cultered from newborn WT and *Nrx3*$^{SS4+}$ mice as described (Kaeser et al., 2011), infected on DIV4-5 with lentiviruses, and analyzed at DIV13-16. Rescue experiments were performed by concurrent superinfection of neurons with the rescue virsuses. For transfections of neurons, we employed the calcium phosphate method (Matus et al., 2007).

Stereotactic injections. WT and *Nrx3*$^{SS4+}$ mutant mice on an SV129/Bl6 hybrid background were anesthetized with tribromoethanol (125-200 mg/kg) at P21. AAV was injected with a glass pipette bilaterally with two locations per hemisphere into the CA1 region of the hippocampus (Bregma coordinates: AP: -1.95/-2.20 mm, ML: ±1.12/±1.20 mm, DV: -1.20/-1.30; flow rate = 0.15 □l/min; injected volume = 0.85 μl). Efficiency and localization of AAV expression was confirmed by nuclear GFP expression of inactive and active GFP-Cre recombinase fusion protein expression by histochemistry.

Histochemistry. Mice were anesthetized with tribromoethanol and perfused with 10 ml PBS followed by 25-30 ml fixative (4% paraformaldehyde PBS). Brains were removed and postfixed in 30% sucrose PBS overnight. Fixed tissued was sectioned at 35 μm before being mounted on glass slides with Fluoromount-G (SouthernBiotech; Birmingham, AL). Stitched images were taken on an Olympus a BX53 and acquired using Olympus VS120 software.

Electrophysiology. Whole-cell patch-clamp recordings from cultured neurons were performed as described using 3-4 MΩ pipettes (WPI) (Aoto et al., 2007; Maximov et al., 2007). Cultures were continuously superfused with extracellular solution (ACSF; in mM): 126 NaCl, 2.5 KCl, 1 NaH_2PO_4, 26.2 $NaHCO_3$, 2.5 $CaCl_2$, 1.3 $MgSO_4$-7 H_2O, 11 D-Glucose, ~290 mOsm. mEPSCs and EPSCs were recorded with an internal solution containing (in mM): 117 Cs-methanesulfonate, 15 CsCl, 8 NaCl, 10 TEA-Cl, 0.2 EGTA, 4 Na_2-ATP, 0.3 Na_2-GTP, 10 HEPES, pH 7.3 with CsOH (~300 mOsm). A constant hyperpolarizing current was used to maintain a resting potential of -60 to -70 mV. mIPSCs and IPSCs were recorded filled with an internal solution containing (in mM): 145 CsCl, 5 NaCl, 10 HEPES-CsOH pH 7.3, 10 EGTA, 4 Na_2-ATP, and 0.3 Na_2GTP (~300 mOsm), without (mIPSCs) or with (IPSCs) 10 QX-314. mEPSCs and mIPSCs were recorded in 0.5 μM tetrodotoxin (TTX) plus either 100 μM picrotoxin (mEPSCs) or 10 μM 6-cyano-7-nitroquinoxaline-2,3-dione (CNQX) and 50 μM D-(-)-2-amino-5-phosphonopentanoic acid (D-APV; mIPSCs), respectively. Miniature events were handpicked and analyzed in Clampfit 10 (Molecular Devices) using template matching and a threshold of 5 pA. Evoked synaptic currents were elicited with a bipolar stimulating electrode (A-M Systems, Carlsborg, WA) placed 100-150 μm from the soma of recorded neurons,and controlled by a Model 2100 Isolated Pulse Stimulator (A-M Systems, Inc.) synchronized with the Clampex 10 data acquisition software (Molecular Devices). After formation of the whole-cell configuration and equilibration of the internal solution, the series resistance was compensated to 5-8 MΩ. To isolate individual glutamatergic and GABAergic currents, evoked responses were recorded in 100 μM picrotoxin and 50 μM D-APV (AMPAR), 100 μM picrotoxin and 10 μM CNQX (NMDAR), and 10 μM CNQX and 50 μM D-APV (IPSCs). Synaptic currents were monitored with a Multiclamp 700B amplifier (Molecular Devices). Data were collected at 10 kHz and filtered with a lowpass filter at 2 kHz. For all experiments, the experimenter was blind to the recording condition.

For acute slice electrophysiology, wildtype and mutant mice were used 2-3 weeks after infection. Transverse hippocampal slices (300□m) were cut in ice-cold solution containing (in mM): 85 NaCl, 75 Sucrose, 2.5 KCl, 1.3 NaH_2PO_4, 24 $NaHCO_3$, 0.5 $CaCl_2$, 4 $MgCl_2$, 25 D-Glucose saturated with 95% O_2/5% CO_2. Slices were transferred to a holding chamber containing artificial cerebrospinal fluid (ACSF, in mM): 126 NaCl, 2.5 KCl, 1 NaH_2PO_4, 26.2 $NaHCO_3$, 2.5 $CaCl_2$, 1.3 $MgSO_4$-7H_2O, 11 D-Glucose, ~290 mOsm. Slices were allowed to recover at 31.5º C for 30 min then at room temp for 1 hr. Acute slices where transferred to a recording chamber continuously superfused with oxygenated ACSF (1.5 ml/min) maintained at 30.5º C. For AMPAR:NMDAR ratio and LTP experiments, 50 μM picrotoxin was added. For whole-cell input/output measurements and control LTP experiments, 50 μM picrotoxin and 100 μM D-APV was added. Whole-cell voltage-clamp recordings were made with 2.5-3 MO borosilicate glass pipettes (WPI) filled with the following internal solutions (in mM): for AMPAR:NMDAR measurements: 117 Cesium-Methanesulfonate, 15 CsCl, 8 NaCl, 10 TEA-Cl, 0.2 EGTA, 4 Na_2-ATP, 0.3 Na_2-GTP, 10 HEPES, 5 Phosphocreatine pH 7.3 with CsOH, ~300 mOsm; for input/output, PPR, and LTP experiments: 137 K-gluconate, 5 KCl, 10 HEPES, 4 ATP-Mg_2, 0.5 GTP-Na_2, 10 Phosphocreatine, 0.2 EGTA, pH 7.2 with KOH. Neurons were clamped at -65 mV for recording extracellular-evoked EPSC in hippocampal slices and EPSCs were evoked by alvear stimulation. Depolarizing current steps were applied to characterize the cells firing behavior. To measure NMDAR current, cells were clamped at +40 mV. To calculate the AMPAR to NMDAR ratio, the peak AMPAR amplitude was measure as was the NMDAR current at 40 ms following the peak EPSC. Paired-pulse values were collected at inter-stimulus

intervals ranging from 20 ms to 2 sec. LTP in the subiculum was analyzed as previously described (Wozny et al., 2008). Briefly, a nichrome stimulating electrode was placed at the distal border of CA1. Four tetani of high-frequency stimulation were applied in current-clamp mode at resting membrane potential at 100 Hz for 1 sec with 10 sec intertrain intervals. Baseline and post-LTP induction EPSCs were sampled at 0.1 Hz and binned into 1 min epochs. The magnitude of LTP was assessed by averaging the last 10 min of each experiment (50-60 min after induction). Paired-pulse ratios were then measured after the termination of LTP recording (60 min after induction) at ISIs ranging from 20 ms to 2 sec.

Statistics. All values are represented by the average of independent experiments ± SEM. Statistical significance for electrophysiological experiments was determined by single-factor ANOVA. Significance of weight distribution was determined by 2-way ANOVA. Statistical analyses of cumulative probabilities were performed by the Kolmogorov-Smirnov test (K-S test) from: http://www.physics.csbsju.edu/stats/KS-test.n.plot_form.html.

SUPPLEMENTAL REFERENCES

Aoto, J., Ting, P., Maghsoodi, B., Xu N., Henkemeyer, M., and Chen, L. (2007). Postsynaptic ephrinB3 promotes shaft glutamatergic synapse formation. J Neurosci *27*, 7508-7519.

Aoto, J., Nam, C.I., Poon, M.M., Ting, P., and Chen, L. (2008). Synaptic signaling by all-trans retinoic acid in homeostatic synaptic plasticity. Neuron *60*, 308-320.

Carroll, R.C., Lissin, D.V., von Zastrow, M., Nicoll, R.A., and Malenka, R.C. (1999). Rapid redistribution of glutamate receptors contributes to long-term depression in hippocampal cultures. Nat Neurosci *2*, 454-460.

Kaeser, P.S., Deng, L., Wang, Y., Dulubova, I., Liu, X., Rizo, J., and Südhof, T.C. (2011). RIM proteins tether Ca^{2+} channels to presynaptic active zones via a direct PDZ-domain interaction. Cell *144*, 282-295.

Lin, J.W., Ju, W., Foster, K., Lee, S.H., Ahmadian, G., Wyszynski, M., Wang, Y.T., and Sheng, M. (2000). Distinct molecular mechanisms and divergent endocytotic pathways of AMPA receptor internalization. Nat Neurosci *3*, 1282-1290.

Matus, A., Biou, V., Brinkhaus, H., and Roelandse, M. (2007). Transfecting Cultured Hippocampal Neurons with an Actin-GFP Plasmid. CSH Protoc *2007*, pdb prot4664.

Maximov, A., Pang, Z.P., Tervo, D.G., and Südhof, T.C. (2007). Monitoring synaptic transmission in primary neuronal cultures using local extracellular stimulation. J Neurosci Methods *161*, 75-87.

Pang, Z.P., Bacaj, T., Yang, X., Zhou, P., Xu, W., and Südhof, T.C. (2011). Doc2 supports spontaneous synaptic transmission by a Ca^{2+}-independent mechanism. Neuron *70*, 244-251.

Tabuchi, K., Blundell, J., Etherton, M.R., Hammer, R.E., Liu, X., Powell, C.M., and Südhof, T.C. (2007). A neuroligin-3 mutation implicated in autism increases inhibitory synaptic transmission in mice. Science *318*, 71-76.

Tabuchi, K., and Südhof, T.C. (2002). Structure and evolution of neurexin genes: insight into the mechanism of alternative splicing. Genomics *79*, 849-859.

Wozny, C., Maier, N., Schmitz, D., and Behr, J. (2008). Two different forms of long-term potentiation at CA1-subiculum synapses. J Physiol *586*, 2725-2734.

Xu, W., Morishita, W., Buckmaster, P.S., Pang, Z.P., Malenka, R.C., and Südhof, T.C. (2012). Distinct neuronal coding schemes in memory revealed by selective erasure of fast synchronous synaptic transmission. Neuron *73*, 990-1001.

Supplemental Figure 1

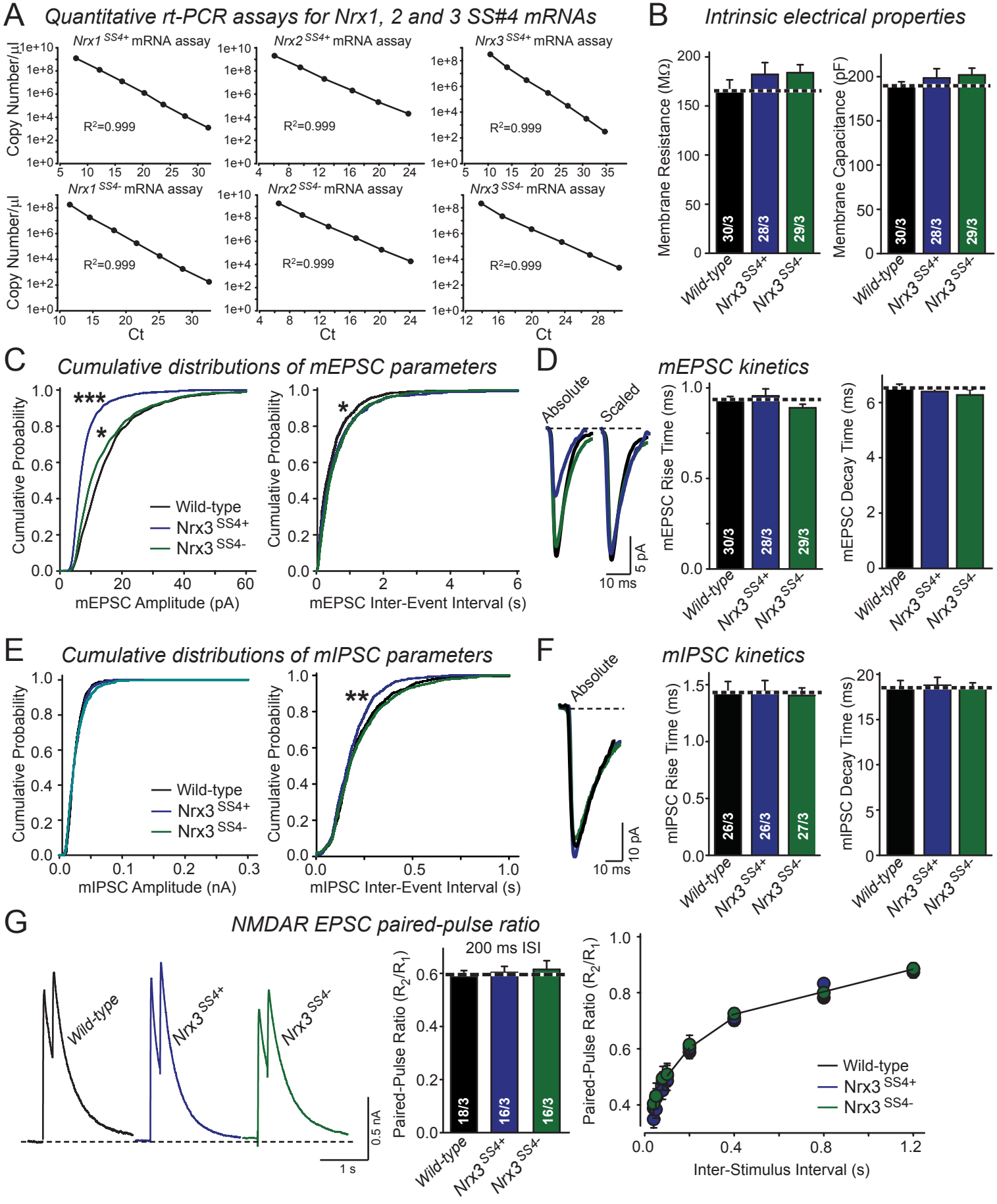

Supplemental Figure 2

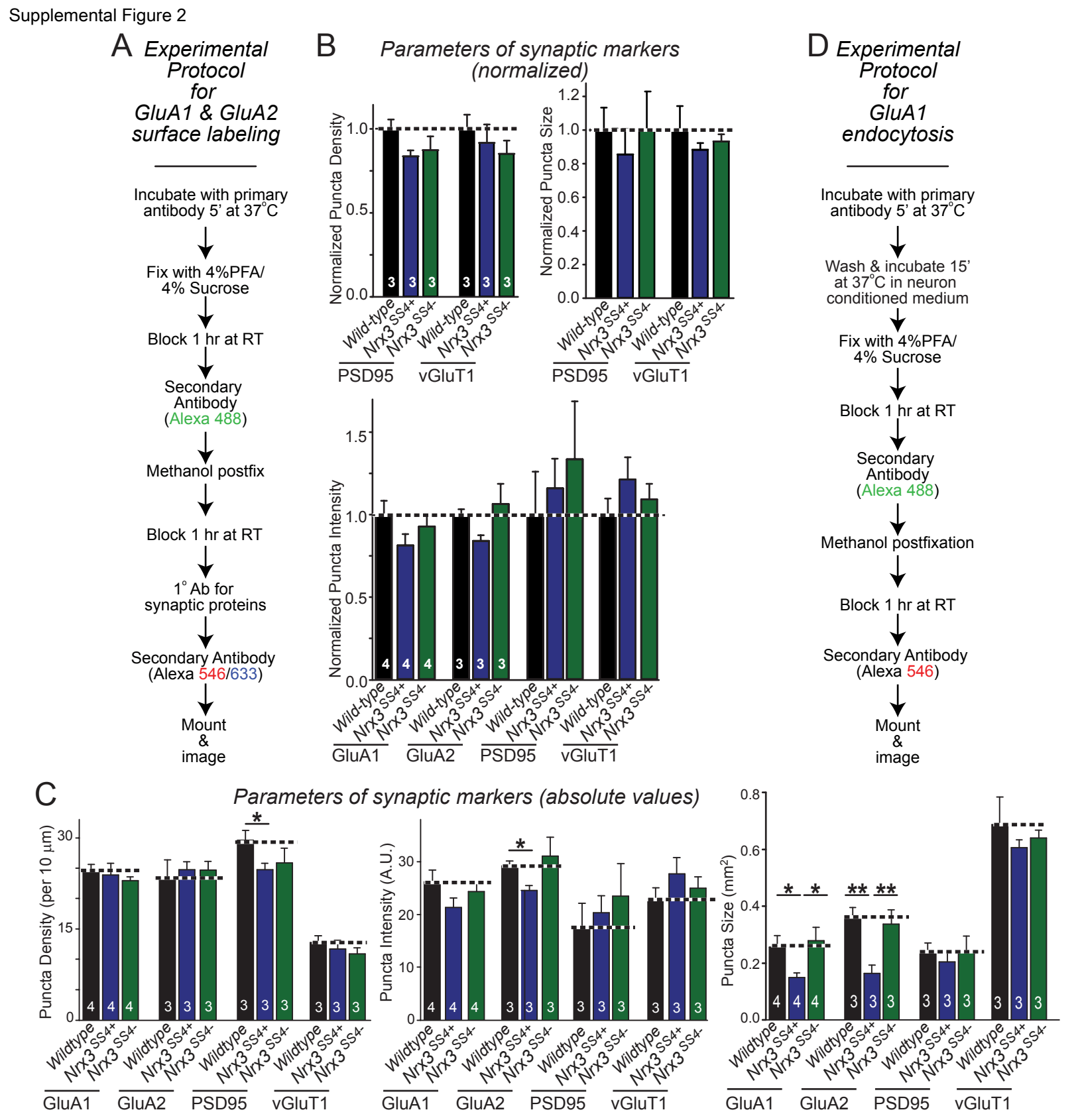

Supplemental Figure 3

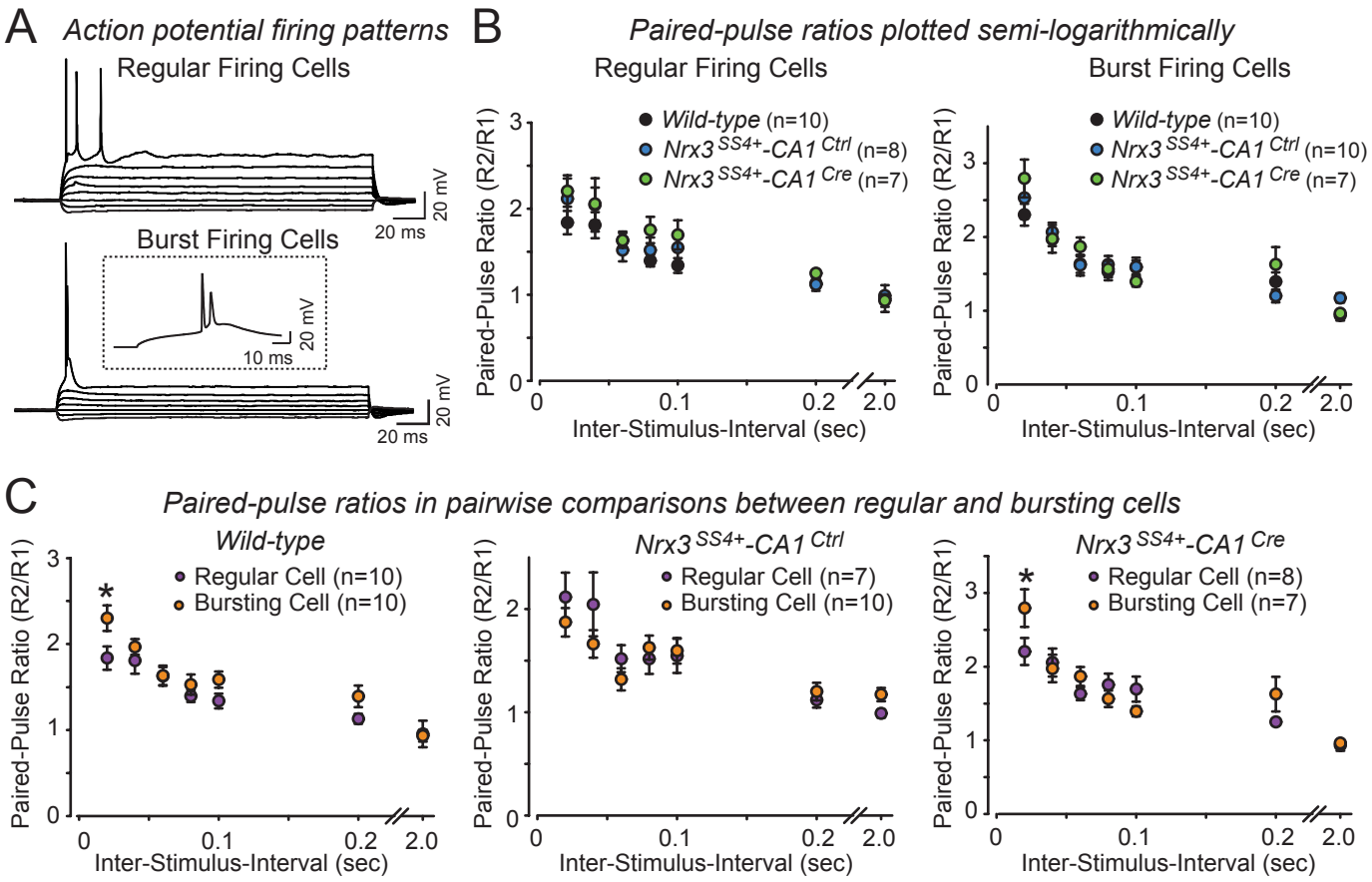

Supplemental Figure 4

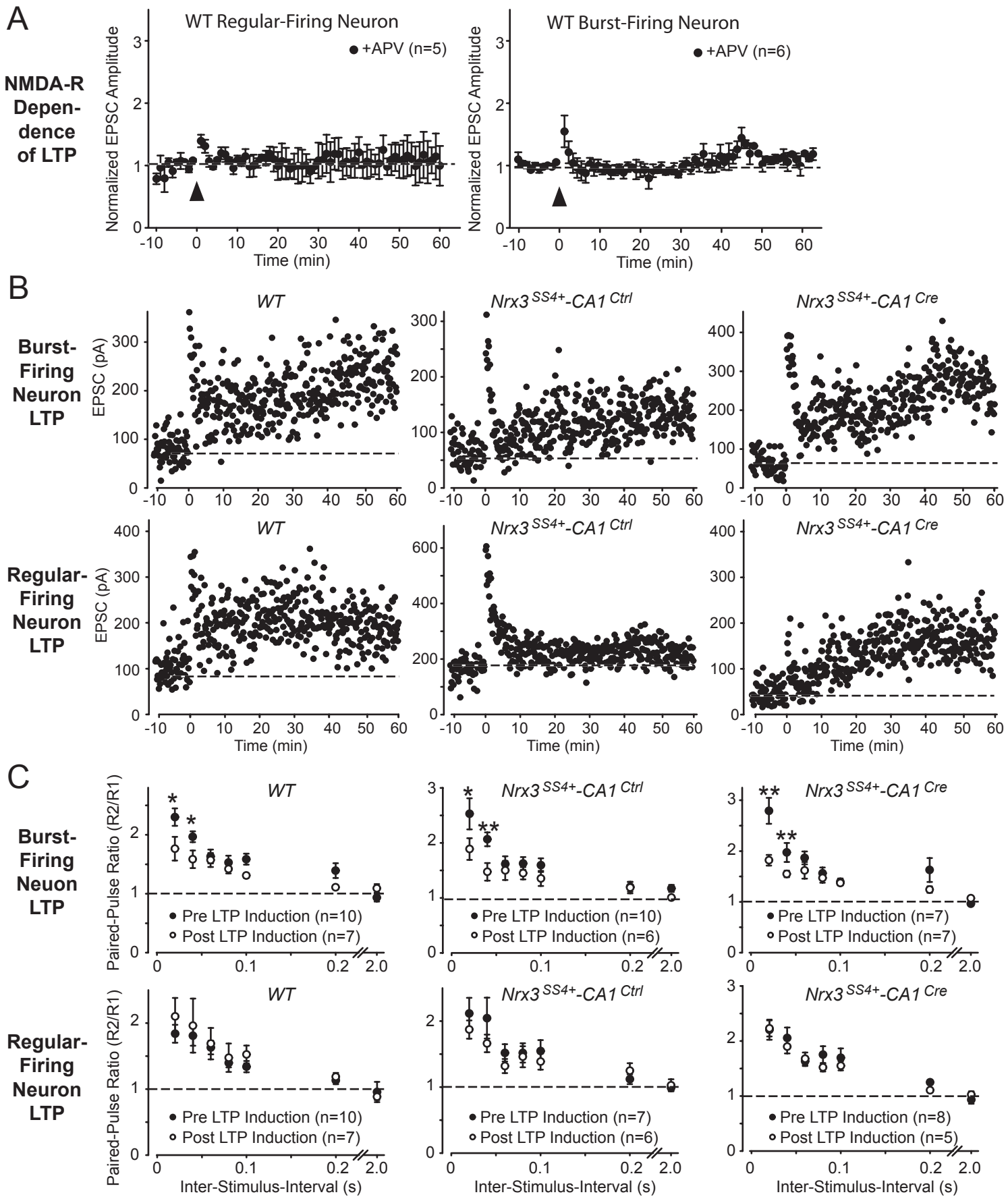

Supplemental Figure 5

A